Available online at www.sciencedirect.com
SCIENCE DIRECT
Surface & Coatings Technology 200 (2005) 1315–1319
SURFACE & COATINGS TECHNOLOGY
www.elsevier.com/locate/surfcoat

The influence of the period size on the corrosion and the wear abrasion resistance of TiN/Ti multilayers

M. Flores [a,*], S. Muhl [b], L. Huerta [b], E. Andrade [c]

[a] Departamento de Ingeniería de Proyectos, CUCEI, Universidad de Guadalajara, J. Guadalupe Zuno 48, Los Belenes, Zapopan Jal., 45101, México
[b] Instituto de Investigaciones en Materiales, UNAM, Ciudad Universitaria, Coyoacan, A.P. 70-36, México D.F., 04510, México
[c] Instituto de Física, UNAM, A.P. 20-364, México, D. F., 01000, México

Available online 21 October 2005

Abstract

Metal-ceramic multilayers were deposited by reactive magnetron sputtering with the aim to simultaneously improve the corrosion and wear resistance of metallic substrates. In this paper we report the results of studies of the influence of the period size on the corrosion and the wear abrasion resistance of TiN/Ti multilayers deposited on H13 steel substrates. The Ti layers were deposited with thickness between 19 and 150 nm and TiN deposited with 22–150 nm; the number of periods was from 1 to 60. The wear was studied using a commercial ball cratering system and the corrosion with potentiodynamic polarizations in an electrolyte of NaCl 0.5 M. It was found that reducing the period also decreased the grain size and that the wear resistance of multilayer was improved; however the results of the corrosion testing were somewhat mixed. The results obtained for the periodic multilayers are compared with monolithic films. XRD analysis was used to study the influence of the period on the grain size and texture of the multilayers. Ion beam methods (RBS) were used to obtain the atomic composition profiles and the TiN/Ti multilayer thickness.

Keywords: Metal ceramic multilayers; corrosion; wear

1. Introduction

Nitride hard coatings such as TiN are extensively used to improve the tribological properties of less noble materials such as steels. The coated parts are frequently exposed to a corrosive environment during use and in these cases the system can fail because the permeable coating allows the corrosive medium to reach the metallic substrate. This corrosive attack is due to imperfections within the coating, associated with microcracks, pores, pinholes, transient grain boundaries, and the common columnar morphology of monolithic PVD-deposited films. Multilayers are a way to improve the corrosion and tribological properties, but some film characteristics such as the stress and grain size have the opposite effect on the above-mentioned properties. There exist complex applications such as surgical implants and prosthesis where it is necessary to protect the metallic substrate simultaneously against wear and corrosion. The mechanical and tribological properties of Ti–TiN have been studied in the last decade [1–6] but the corrosion properties have received less attention [7–9]. The unique combination of properties achieved in multilayers promises new applications in fields such as superhard coatings for dry machining, substitution of electrochemical thick coatings and to produce freestanding multilayer foils, where the properties of monolithic layers are exceeded [10–12]. There are only few reports that analyzed both properties simultaneously [13–15] and there is a need for studies about the effects of period on these properties. In this work we have studied the effect of period size on the corrosion and abrasive wear resistance for samples deposited by magnetron sputtering. We also report the texture and grain size variation as a function of the period size.

2. Experimental details

2.1. Coating deposition

The substrates were made of cut pieces of rolled and annealed commercial plate (AISI H13) steel without post

* Corresponding author. Tel.: +52 33 3836 4500; fax: +52 33 3836 4502.
E-mail address: maflores@newton.dip.udg.mx (M. Flores).

0257-8972/$ - see front matter © 2005 Elsevier B.V. All rights reserved.
doi:10.1016/j.surfcoat.2005.08.115

thermal treatment. Samples, $2.54 \times 7.62 \times 1.27$ cm^3, were polished using 2000 sandpaper and finished with 1 and 0.5 μm diamond paste. Prior to deposition the substrates were ultrasonically cleaned first in acetone and then in alcohol.

The multilayer coatings were deposited by magnetron sputtering using a 10.20 cm diameter titanium target (99.99% purity). An argon plasma was used for the titanium layers for 0.5 to 4 min on each layer at a pressure of 0.27 Pa and an atmosphere of argon (41.6%) plus nitrogen (58.4%) for the titanium nitride layers for 0.5 to10 min on each layer at a pressure of 0.53 Pa as detailed in Table 1. The plasma current for Ti deposition was 0.4 A and for TiN 0.45 A. In the multilayers the deposition rate for TiN was 0.25 ± 0.05 and 0.625 ± 0.13 nm/s for Ti. For the six-period multilayer, each layer was 150 ± 30 nm thick. The temperature of the substrates was maintained at 450 °C and the substrates were placed 5 cm in front of the target. The change from Ti to TiN deposition was achieved by controlling the nitrogen flow (Ar: 4 sccm, N_2: 5.6 sccm) without plasma interruption so that a graded interface was generated. For all the specimens the first deposited layer was of Ti and the last of TiN. A bilayer sample with a Ti layer, 180 nm thick, and a TiN layer of 1.6 μm (120 min) was prepared as a reference. It was found that in the deposition of the TiN monolayer the deposition rate was reduced possibly due to an increase in the target poisoning which in the case of the multilayers is less important since the Ar plasma used for each Ti layer effectively cleans the target. The number of periods and modulation of the multilayers are described in Table 1. The changes in the voltage for the samples with 18 and 60 periods is due to the use of a new target and the higher voltages used for the samples prepared using magnetic enhancement are due to the modification that this produces in the performance of magnetron. There are two groups of samples, one deposited with the substrate grounded of multilayers of 1, 6 18 and 60 periods and the second of multilayers of 6 and 12 periods deposited with the substrates polarized. The magnetic field of the magnetron was enhanced with a coil to produce the unbalanced condition. The details of the changes produces by the coil on the magnetic field and the plasma characteristic were published elsewhere [16].

Table 1
Deposition parameters of TiN/Ti multilayers of grounded samples

Total thickness (nm)	Number of periods	Ti thickness (nm)	TiN thickness (nm)	Plasma voltage Ti (V)	Plasma voltage TiN (V)
1880	1	180	1700	410	420
1800	6	150	150	405	420
1494	18	38	45	510	490
2460	60	19	22.5	510	490
Samples with bias of −100 V and an additional magnetic field at a coil current of 10 A					
1800	6	150	150	680	570
1800	12	75	75	680	585

2.2. Wear tests

A ball cratering system was used to measure the wear resistance of the multilayers. In each case, eight wear tests were performed on each of two samples deposited under the same conditions and we report the average value obtained. The ball used was 3 cm in diameter of steel coated with chromium. The velocity was 100 rpm and the total distance travelled was 9.425 m (100 revolutions). The load used was 1 N and the abrasive was a diamond colloid with a particle size of 0.1 μm. The volume lost by the wear in the crater V_C was obtained from the depth h of the crater and the radius of the ball, $V_C = \frac{1}{3}\pi h^2(3R_b - h)$ where R_b is the radius of the ball. The depth of the crater was calculated from the measurement of the largest diameter D of the crater using the relation, $h = 1.5\ \text{cm} - \sqrt{2.25\ \text{cm}^2 - (D/2)^2}$.

2.3. Corrosive tests

The samples used for the corrosion tests were cut from the same samples used for the wear test. The corrosion resistance of the TiN/Ti coatings was evaluated by potentiodynamic polarization scans in a 0.5 M NaCl solution. The electrolyte used was an aerated solution prepared from reagent grade NaCl and distilled water. The potential sweep rate was 10 mV/min at 22 °C. The walls of the samples were double-painted with enamel, except for an area of 1 cm^2. The corrosion current density i_{corr} was found from a Taffel extrapolation of the anodic zone of the semilogaritmic plot [17]. The reproducibility of the results was checked by performing polarizations of, at least, three samples under the same conditions and the most typical result of these is reported.

2.4. Coatings characterization

A stylus profilometer and the ball cratering systems were used to measure the thickness and roughness and from these the deposition rate of the layers was calculated. The film structure and preferred growth orientation were determined using a Siemens D500 X-ray diffractometer with Cu Kα radiation. The grain size was calculated using the relation $t = 0.9\lambda / B\cos\theta$, $B^2 = B_M^2 - B_s^2$, where B is the broadening of diffraction line, B_M is the measured width of the diffraction line (width of the integral of the diffraction line produced by the (200) plane of TiN), $B_s = 0.21$ is the width of a diffraction line from a single crystal silicon substrate and θ is the angle of the position of maximum intensity of the diffraction line. The ion beam analysis (IBA) facilities of the Universidad Nacional Autonoma de Mexico were used to obtain the atomic composition of TiN/Ti layers, as well as the concentration depth profiles. A 1380 keV deuterium beam was used to bombard the samples. A surface barrier detector, 1000-μm thick, equipped with standard electronics set at $\theta = 150°$ angle was used to measure the energy of the particles. A combination of RBS plus NRA was applied to evaluate the samples' energy spectra. The $^{14}N(d,\alpha_1)^{12}C$ NR cross sections are well known and were used as way to determine the N concentration in the TiN layers [18].

3. Results and discussion

3.1. Microstructure and composition of the multilayers

The XRD diffraction pattern shown in Fig. 1a indicates that, for the case of the multilayers, the preferential orientation of TiN was in the directions (111) and (200) without important changes as the period size was reduced. The diffraction line corresponding to the TiN (200) plane became broader as the period size decreased. The calculation of the variation of the interplanar distance of the planes (200) of TiN shows that as the periods was reduced the d value was closer to the value of d_{200}=0.21208 nm for bulk TiN. The calculated grain size decreased as the thickness of the TiN layer was reduced as shown in Fig. 1b. In the case of the bias multilayers the grain size was 18 nm for the 6-period multilayers and 22 nm for the 12-period multilayer; this indicates that the dominant effect is the bias rather than the period size.

The IBA studies showed that, within the experimental error, the composition of the TiN layers was stoichiometric: 50% N and 50% Ti, that interfaces were graded and that the interface between the TiN and Ti was more extended than that between the Ti and TiN. XPS and AES analysis, using a TiN standard, confirmed the composition of the TiN films obtained by IBA.

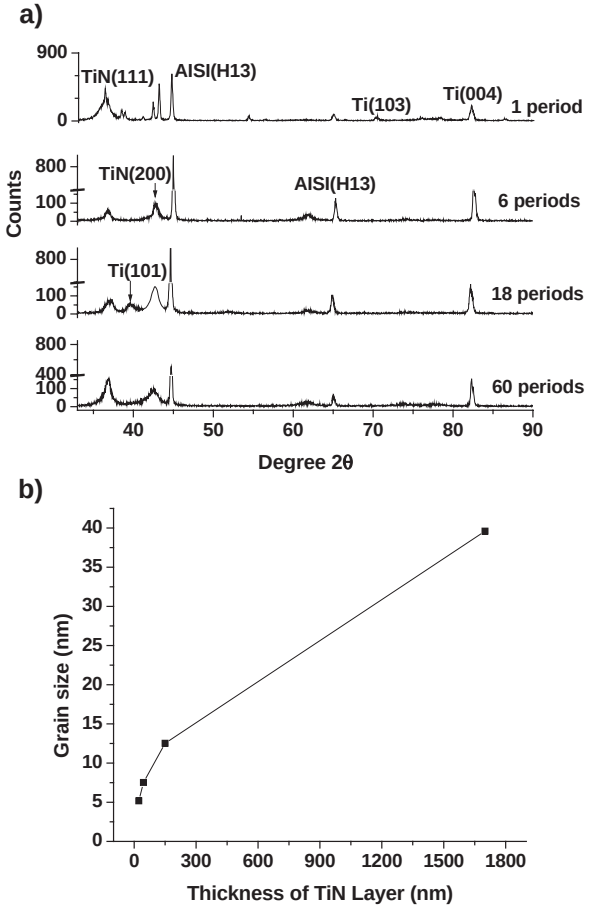

Fig. 1. a) The XRD pattern of samples deposited with different period sizes. b) The calculated grain size as a function of the deposition time of the TiN layer.

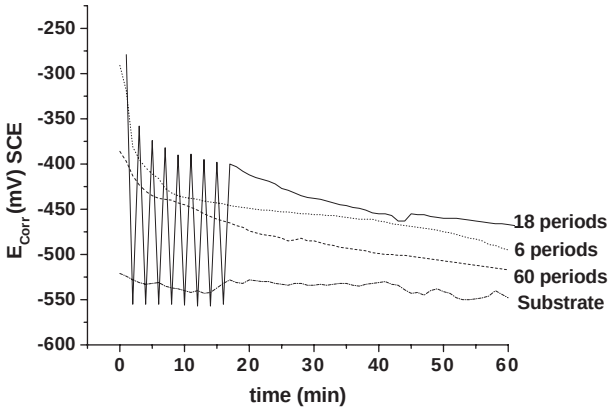

Fig. 2. The temporal evolution of the corrosion potential, E_{corr}, for the grounded multilayers.

3.2. Corrosion results of the grounded multilayers

Fig. 2 shows the evolution in time of corrosion potential E_{corr}, all the layers had potentials more noble than the substrate, and the multilayer with 60 periods had the most active potential of the three multilayers; this indicated its tendency to corrode. The sample with 18 periods showed cyclic activation–passivation behaviour for the first 17 min and afterwards to the end of measurement it showed a reduced tendency to corrode.

Typical curves of the potential-current density using a semi-logarithmic scale are shown in the Fig. 3. A comparison of the curves reveals that in the cathodic part, starting from −800 mV, there is a tendency to higher cathodic current values as the number of periods increased and the individual layer thickness decreased. These can be explained by the reduction of the grain size observed in these samples. In the anodic zone for potentials beyond −150 mV the tendency is inverted; the corrosion current is higher for the samples with less periods which is an indication that the kinetics of corrosion are dominant. A similar behaviour has been reported for ion etching of multilayers. All multilayers are almost equally noble in the cathodic zone but the multilayers with more periods have the lower final corrosion current [19]. In Table 2 we show the corrosion current calculated from the

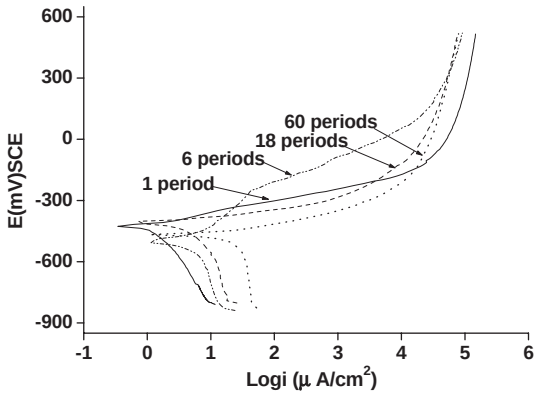

Fig. 3. Polarization curves, in 0.5 M NaCl solution, of the grounded TiN/Ti multilayers as a function of the number and size of the periods.

Table 2
Electrochemical parameters of grounded multilayers

Periods	E_{corr} (mV)	i_{corr} (μA/cm2)	i (E=500 mV) μA/cm^2
60	−469	10	7.7×10^4
18	−496	5	7.5×10^4
6	−405	2	8.7×10^4
1	−425	1	14.4×10^4

Taffel extrapolation and those for a potential at end of polarization. The lowest corrosion current at 500 mV indicates that the best final corrosion resistance of the multilayers was for those with more periods and greater thickness.

3.3. Wear results of grounded multilayers

Fig. 4 shows the results of abrasive wear measurements of the grounded samples with periods between 1 and 60. The lost volume decreased as the period number increased, which can be explained by the grain size reduction as the period size decreased. The grain boundaries and the layer interfaces act as barriers to crack propagation [20]. The multilayers with both of these characteristics showed increased resistance to material loss.

3.4. Wear and corrosion resistance of bias and magnetic field enhanced multilayers

Fig. 5 shows the shift in the (111) TiN diffraction peaks of the 6- and 12-period multilayer samples relative to the position of this peak found in bulk α-fcc TiN. The shift can be seen to be greater for the 12-period sample. Fig. 6a shows the volume lost in the wear abrasive test for the multilayers with 6 and 12 periods. In these multilayers the substrate was biased and the magnetic field of the magnetron enhanced with a coil. Since the grain size was almost constant the increased wear resistance can be explained by the increased residual stress that is indicated by the shift of the diffraction lines. Fig. 6b shows the curves of the potentiodynamic polarization; in this case the multilayers with less interfaces have better corrosion resistance. This is in good agreement with the increase of the stress. This is opposite to the grounded multilayer case, where dominant effect was the number of interfaces instead of the amount of stress. The effect of the bias is to increase the energy of the ions bombarding the film during growth and the magnetic enhancement modifies the ion-to-atomic ratio and the energy per deposited atom (these results will be published elsewhere). The ion energy obtained with polarization (about 100 eV) can produce defects and stresses and, for this experimental range, the effect of this on the corrosion is greater than the reduction of period size.

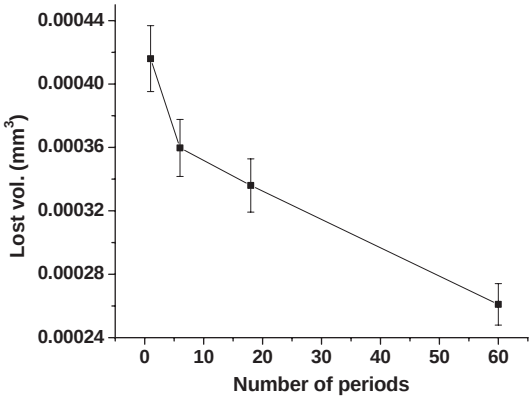

Fig. 4. Abrasive wear of the grounded multilayers as a function of the number of periods.

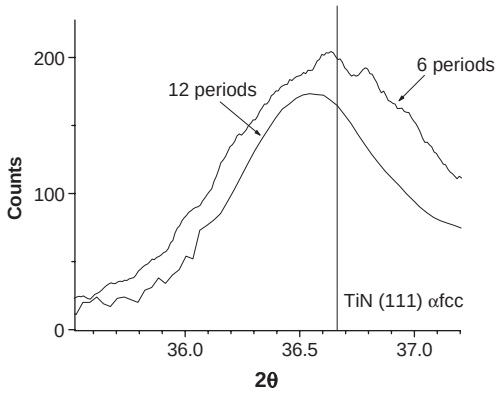

Fig. 5. The shift of the diffraction line of (111) TiN plane for the biased multilayers of 6 and 12 periods; the solid line indicates the position of this peak in bulk TiN.

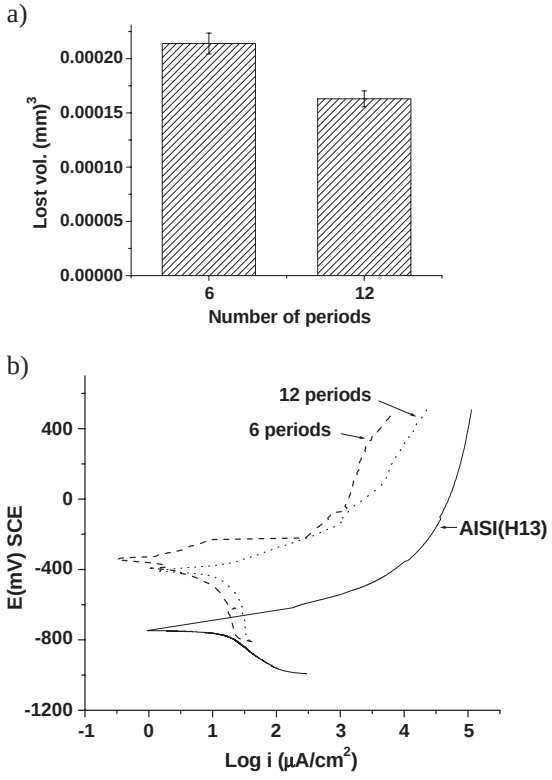

Fig. 6. a) The abrasive wear of the multilayers deposited with additional magnetic field and a biased substrate for 6 and 12 periods. b) The polarization curves in 0.5 M NaCl solution of the same samples.

4. Conclusion

The grain size of the TiN layers of the grounded multilayers decreased as the individual thickness decreased and this was found to increase the wear resistance. In the case of corrosion when the period size was decreased, there was an increased tendency to corrode at the beginning of the test in the cathodic zone induced by the grain size reduction, but this behaviour was inverted in the anodic zone for higher potentials. This may be due to the fact that the corrosion kinetics are controlled by the layer interfaces and, since it is this that produces the final corrosion resistance, the multilayers with more interfaces are better at resisting corrosion.

The grain size for the biased multilayers is almost constant for the period size variation: from 300 to 150 nm. For this change of period, it was found that there was a reduction in the corrosion resistance and an increase in the wear resistance and this is considered to be due to an increase in the induced residual stress.

Acknowledgments

Financial assistance by the Propesti program of the University of Guadalajara is greatly acknowledged. The authors wish to thank Leticia Baños for the XRD measurements and to E.P. Zavala for his assistance with the RBS analysis.

References

[1] M. Bromarks, M. Larsson, P. Hedenqvist, S. Hogmark, Surf. Coat. Technol. 90 (1997) 217.
[2] C. Sant, M.B. Daia, P. Aubert, S. Labdi, P. Houdy, Surf. Coat. Technol. 127 (2000) 167.
[3] T.S. Li, H. Li, F. Pan, Surf. Coat. Technol. 137 (2001) 225.
[4] H.A. Jehn, Surf. Coat. Technol. 131 (2000) 433.
[5] E. Kusano, M. Kitagawa, H. Nanto, A. Kinbara, J. Vac. Sci. Technol., A, 16 (3) (1998) 1272.
[6] Duck, N. Gamer, W. Gesatzke, M. Griepentrog, W. Osterle, M. Sahre, I. Urban, Surf. Coat. Technol. 142–144 (2001) 579.
[7] M. Herranen, U. Wiklund, J.O. Carlsson, S. Hogmark, Surf. Coat. Technol. 99 (1998) 191.
[8] M. Lakatos, D. Hanzel, Corros. Sci. 41 (1999) 1585.
[9] C. Liu, A. Leyland, Q. Bi, A. Matthews, Surf. Coat Technol. 141 (164–173) (1998) 164.
[10] S. Veprek, M. Jilek, Pure Appl. Chem. 74 (3, 475) (2002) 481.
[11] B. Navinsek, P. Panjan, I. Milosev, Surf. Coat. Technol. 116–119 (1999) 476.
[12] M.G. Brookes, P.J. Kelly, R.D. Arnell, Surf. Coat. Technol. 177–178 (2004) 518.
[13] R. Hubler, A. Cozza, T.L. Marcondes, R.B. Souza, F.F. Fiori, Surf. Coat. Technol. 142–144 (2001) 1078.
[14] R. Hubler, Nucl. Instrum. Methods Phys. Res., B Beam Interact. Mater. Atoms 175–177 (2001) 630.
[15] E. Vera, G.K. Wolf, Nucl. Instrum. Methods Phys. Res., B Beam Interact. Mater. Atoms 148 (1999) 917.
[16] M. Flores, S. Muhl, E. Andrade, Thin Solid Films 433 (2003) 217.
[17] A.J. Bard, L.R. Faulkner, Electrochemical Methods: Fundamentals and Applications, John Wiley & Sons, 2001, p. 103.
[18] E. Andrade, M. Flores, S. Muhl, N.P. Barradas, G. Murillo, E.P. Zavala, M.F. Rocha, Nucl. Instrum. Methods Phys. Res., B Beam Interact. Mater. Atoms 219–220 (2004) 763.
[19] M. Fenker, M. Balzer, H.A. Jehn, H. Kappl, J.J. Lee, K.H. Lee, H.S. Park, Surf. Coat. Technol. 150 (2002) 101.
[20] G.S. Was, T. Foecke, Thin Solid Films 286 (1996) 1.